BJR
© 2017 The Authors. Published by the British Institute of Radiology
https://doi.org/10.1259/bjr.20160561

Received: 22 June 2016 | Revised: 23 January 2017 | Accepted: 11 July 2017

Cite this article as:
Granata V, Fusco R, Catalano O, Filice S, Avallone A, Piccirillo M, et al. Uncommon neoplasms of the biliary tract: radiological findings. *Br J Radiol* 2017; **90**: 20160561.

FULL PAPER

Uncommon neoplasms of the biliary tract: radiological findings

[1]VINCENZA GRANATA, MD, [1]ROBERTA FUSCO, PhD, [1]ORLANDO CATALANO, MD, [1]SALVATORE FILICE, MD, [2]ANTONIO AVALLONE, MD, [3]MAURO PICCIRILLO, MD, [3]MADDALENA LEONGITO, MD, [3]RAFFAELE PALAIA, MD, [4]ROBERTO GRASSI, MD, [3]FRANCESCO IZZO, MD and [1]ANTONELLA PETRILLO, MD

[1]Division of Radiology, Istituto Nazionale Tumori IRCCS Fondazione Pascale, IRCCS di Napol, Naples, Italy
[2]Division of Abdominal Oncology, Istituto Nazionale Tumori IRCCS Fondazione Pascale – IRCCS di Napoli, Naples, Italy
[3]Division of Hepatobiliary Surgical Oncology, Istituto Nazionale Tumori IRCCS Fondazione Pascale – IRCCS di Napoli, NaplesI, Italy
[4]Division of Radiology, Second University of Naples, Piazza Miraglia, Naples, Italy

Address correspondence to: Dr Roberta Fusco
E-mail: *r.fusco@istitutotumori.na.it*

Objective: To report our cancer centre experience in the biliary tumours incidence other than cholangiocellular-carcinoma, emphasizing the radiological features.
Methods: 197 patients with biliary disease undergoing Gd-EOB-DTPA-enhanced MRI were reviewed. Four radiologists evaluated retrospectively size, structure, anatomical site and signal intensity of lesions on MRI. Enhancement-pattern during the arterial-, portal- and late-phase on ultrasound, CT and MR study was assessed as well as the enhancement pattern during the hepato-biliary-phase on MRI.
Results: 23 patients were selected. The lesion was intraductal in 5 cases, periductal in 14 and intrahepatic in 4. 16 lesions were solid, 5 uniloculated cystic and 2 complex cystic. In five patients the lesion was simple cyst, with a signal intensity in T_1 weighted (T1W) and T_2 weighted (T2W) similar to the gallbladder. In two patients with complex cystic lesion, the solid component was heterogeneously hypointense in T_1 W, hyperintense in T_2 W with a restricted diffusion. The solid component showed heterogeneous contrast-enhancement on CT, MR and ultrasound. The tumour was intrahepatic in two patients, with signal hypointense in T_1 W and hyperintense in T_2 W. Diffusion was restricted. The lesions showed heterogeneous contrast-enhancement. The periductal lesions were hypointense in T_1 W, hyperintense in T_2 W with restricted diffusion. The lesion showed progressive contrast-enhancement. Peribiliary melanoma was hyperintense in T_1 W, hyperintense in T_2 W with restricted diffusion and progressively contrast-enhanced.
Conclusion: Biliary tumours can have a wide spectrum of radiologic appearances and consequently represent a diagnostic challenge for the radiologist.
Advances in knowledge: MRI is the technique of choice in diagnosing biliary tumours, including rare (non-CCC) tumours.

INTRODUCTION

The neoplasms of the biliary tract, excluding cholangiocellular carcinoma (CCC), are rare.[1] These tumours are histologically classified as benign, borderline and malignant. In relation to their structure they are categorized into cystic and solid.[1] Since biliary tract tumours can vary significantly in location, growth pattern and histologic subtype, these lesions can have a wide spectrum of radiologic appearances. Uncommon biliary tumours generally represent a challenge for radiologists, due to the overlapping of their radiological appearance, therefore they require an accurate differential diagnosis.[1] Knowledge of the radiologic features of the various possible biliary tumours, as well as potential mimickers, is important in the accurate diagnosis and management of these tumours, even more in differentiating between neoplastic and non-neoplastic conditions.[2]

Non-invasive imaging techniques, such as ultrasound (US), CT and MRI, are the most common modalities used to image hepatobiliary diseases, playing a critical role in the diagnosis, staging and treatment of patients with biliary tract tumours, providing also relevant information to assess tumour resectability.[3] Although US is sometimes the primary modality used in the evaluation of biliary tumours, the accuracy of US varies according to the equipment and experience of the operator.[4] US is less accurate in the estimation of tumour spread and the determination of tumour resectability compared with CT and MRI.[5,6] CT and MRI are comprehensive imaging modalities with multiplanar capability in the assessment of the liver parenchyma and biliary tree. MRI provides an assessment of the signal characteristics, vascularity and pathophysiology of different tumours because of its superior soft tissue contrast

resolution that includes the use of gadolinium-enhanced techniques.[7,8] Since this information is crucial for tumour staging and treatment planning, MRI is the preferred imaging modality for patients with suspected biliary tumours.[8]

Few studies are available in the literature that provided a comparative and comprehensive analysis of imaging findings of uncommon biliary tumours. Our purpose is to report the experience of a single cancer centre in the incidence of biliary tumours not CCC, emphasizing the radiological features encountered using the different imaging modalities.

METHODS AND MATERIALS

Patient population

Institutional review board approval was obtained for this retrospective study and requirement for informed consent was waived. Through a computerized search of medical records, 197 patients were identified who underwent biliary MR imaging for dilation of the bile ducts and/or jaundice from August 2012 to February 2016. After reviewing the medical records, 15 patients were excluded because they had no disease, 35 patients were not considered because the dilatation was secondary to the presence of stones in the bile ducts, 12 patients were excluded because the dilatation was secondary to lymphadenopathies compressing the bile duct, 32 patients were excluded because the cancer was pancreatic, 25 subjects because the tumour was a CCC, 52 patients because the jaundice was secondary to liver failure (parenchymal metastases). Three other subjects were excluded owing to patient motion artifacts or image noise. The final study population included 23 subjects. For all patients a new computerized search of radiological records was performed to identify which and how many had also been studied with US, CT or contrast-enhanced US (CEUS).

Imaging techniques

MR imaging protocol

MR imaging was performed using a 1.5 T MR (Magnetom Symphony, with Total Imaging Matrix Package, Siemens, Erlangen, Germany) with 8-element body and phased array coils. The MRI examination consisted of basal images taken before IV administration of contrast medium and then functional dynamic sequences obtained after IV injection of liver-specific contrast medium, acquiring the last series of images with a delay of 20 min during the hepatobiliary excretion of the contrast medium. The baseline sequences obtained before IV contrast medium were coronal TRUFISP T_2 weighted free breathing (TR/TE 4.4/2.2 ms, flip angle 80°, slice thickness 4 mm, interval 0 mm, basal resolution 256 mm, phasic resolution 78%, IPAT 2, duration 46 s), axial half-Fourier acquisition single-shot turbo spin-echo (HASTE) T_2 weighted, with controlled respiration, without and with fat-suppressed (FS) gradient-echo puls (Spectral Adiabatic Inversion Recovery—SPAIR) (TR/TE 1500/90 ms, flip angle 170°, slice thickness 5 mm, interval 0 mm, basal resolution 320 mm, phasic resolution 78%, IPAT 2, duration 45 s), coronal HASTE T_2 weighted, without FS (TR/TE 1500/92 ms, flip angle 170°, slice thickness 6 mm, interval 0 mm, basal resolution 320 mm, phasic resolution 70%, IPAT 2, duration 38 s), axial flash in-out phase T_1 weighted, with controlled respiration (TR/TE 160/2,35–4,87 ms, flip angle 70°, slice thickness 5 mm, interval 20%, basal resolution 256 mm, phasic resolution 90%, IPAT 2, duration 33 s), volumetric interpolated breath-hold examination (VIBE) T_1 weighted SPAIR with controlled respiration (TR/TE 4.80/1.76 ms, flip angle 12°, slice thickness 3 mm, interval 20%, basal resolution 320 mm, phasic resolution 70%, IPAT 2, duration 18 s), diffusion-weighted imaging (DWI) with planar echo-pulse sequence (TR/TE 2700/83 ms, slice thickness 3.56 mm, flip angle 90°, acquisition matrix 160 × 102, FOV 136 × 160 mm^2, b value 0, 50, 100, 200, 400, 600 and 800 s mm^{-2}, duration 7.36 min).

The liver-specific gadolinium ethoxybenzyl dimeglumine—EOB (Primovist, Bayer Schering Pharma, Germany) was employed. All patients received 0.1 mL kg^{-1} by means of a power injector (Spectris Solaris® EP MR, MEDRAD Inc., Indianola, IA), at an infusion rate of 1 ml s^{-1}. After completion of the IV injection, VIBE T1-weighted FS (SPAIR) sequences were acquired in five different phases: hepatic arterial- (35 s delay), portal venous- (70 s), late- (90 s), delayed- (120 s) and hepatobiliary excretion phase (20 min).

US and CEUS protocol

CEUS was always preceded by a careful US survey, assessing the size and appearance of the lesion. This baseline assessment was done to appropriately choose the liver area or areas to be particularly focused in the forth- coming contrast-enhanced part of the US study. In all cases, a separated injection was performed for each liver lobe. For both injections, the arterial phase assessment was focused on any known lesion at baseline US. CEUS was performed as a low-mechanical index, double-split mode, real-time modality. A Technos MyLab 70 XVG and MyLab Twice scanner (Esaote, Genoa, Italy) was employed, injecting 2.4 ml of a sulfur hexafluoride-based contrast medium (SonoVue, Bracco, Milan, Italy) for each liver lobe. After the injection, the radiologist focused the sonographic field of view on the parenchymal area of interest, waiting for the microbubbles arrival. Thereafter, the transducer was moved to explore the remaining parenchyma of each lobe, with special reference to the segment bearing the ablated lesion.

CT protocol

Non-contrast phase and contrast-enhanced triple-phase multidetector CT (MDCT) were performed with a 16-detector row scanner (Brilliance 16, Philips Medical Systems, Eindhoven, the Netherlands). MDCT scanning parameters were 120 kVp, 189–200 mAs, 5 mm slice thickness with an increment (overlap) of 2.5 mm and table speed of 18.75–26.75 mm/rotation (pitch 0.828–1.07). Scans were performed in a cranio-caudal direction. Scans were carried out including a region encompassing liver from diaphragm dome to iliac crests as follows: non-contrast phase, hepatic arterial phase scanning began 30–40 s after injection of 120 ml of a non-ionic iodinated contrast media (iomeprol, Iomeron 400, Bracco, Italy) with a bolus triggered technique (120 kVp; 40–60 mA; monitoring frequency from 12 s after the contrast injection; trigger threshold, 100 HUs in the descending aorta). Portal and late phases were obtained scanning the same region, respectively, 70 s and 180 s after contrast medium

injection. The contrast medium was administered at a rate of 4 ml s^{-1} through antecubital vein with an automated injector system (Empower CTA, E-Z-EM Inc., New York, USA).

Images analysis

Four radiologists experts in liver imaging reviewed by consensus all MR, CT and US studies. The radiologists defined peribiliary lesion as a unique when it appeared a single mass of tissue that had grown along the bile ducts, while the lesions were categorized as multiple when more masses were detected. For each lesion the radiologists recorded the size (when possible), the structure, the anatomical site, the signal intensity in T_1 weighted images, T_2 weighted images, DWI and the related map of the apparent diffusion coefficient (ADC). We also evaluated the presence of contrast enhancement during the arterial, portal, late and hepatobiliary phase on MR study, the presence of contrast enhancement during the arterial, portal, late phase on CT study and the presence of contrast enhancement (wash in and wash out) during CEUS study.

The maximum diameter of the lesions, in millimeters, was measured on axial unenhanced T_1 W flash 2D in phase, on unenhanced axial T_1 W flash 2D out phase, on axial HASTE T_2 W, portal phase axial VIBE T_1 W, axial hepatobiliary-phase VIBE T_1 W images, portal phase on CT and CEUS study. According to the structure, the lesions were defined as cystic, complex cystic (with a partial solid component) or solid, while about the location of the lesions, they were classified as intraductal, periductal or intrahepatic. The signal intensity of the lesions in T_1 W and T_2 W images was categorized as isointense, hypointense or hyperintense compared with the surrounding liver parenchyma. The attenuation of the lesions on the CT scans was categorized as isodense, hypodense and hyperdense compared with surrounding liver parenchyma.

We assessed the signal on DWI sequences and measured the ADC of each lesion. When the lesion was visible on all b values this was defined as a restricted diffusion. The diffusion-weighted signal decay was analysed using the mono-exponential model, according to the equation ADC = (ln(S_0/S_b))/b, where Sb is the MRI signal intensity with diffusion weighting b and S0 is the non-diffusion-weighted signal intensity. This analysis was ROI-based using median value of single voxel signals for each b value. ROIs for the tumour were manually drawn to include such hyperintense voxels on image at b value 800 s mm^{-2}. Median diffusion parameters of ROI were used as representative values for each lesion. No motion correction algorithm was used but ROIs were drawn taking care to exclude areas in which movement artifacts or blurring caused voxel misalignments. The data analysis was performed using an in-house code written in Matlab (The MathWorks, Inc., Natick, MA, USA).

We analysed the enhancement pattern during the arterial, portal and late phase on CEUS, CT and MR study and during the hepatobiliary phase of MRI. The enhancement was categorized as homogeneous, heterogeneous, anular (peripheral wash in and central wash out) or target-like (central enhancement with peripheral wash out), as reported a previous study.[9]

Statistical analysis

$\chi 2$ test was employed to analyse differences in largest diameter between T_1 W flash in phase, T_1 W flash out phase, HASTE T_2 W, portal-phase axial VIBE T_1 W, axial hepatobiliary-phase VIBE T_1 W images on MRI and portal-phase axial on CT.

Chi-square test was also employed to analyse differences in size, the anatomical site, the SI in T_1 W images, T_2 W images, in DWI, in the related map of the ADC, the presence of contrast enhancement during the arterial, portal, late and hepatobiliary phase on MR study, the presence of contrast enhancement during the arterial, portal, delayed phase on CEUS and CT. A p value < 0.05 was regarded as statistically significant. Statistical analysis was obtained by means of the Statistic Toolbox of Matlab.

RESULTS

The final study population included 23 patients (12 females and 11 males), with a mean age of 61 years (range 38–80 years). 12 patients (52%) had biliary metastases (five patients with colorectal cancers, three patients had pancreatic cancer, three patients had breast cancer and one patient had gastric cancer), one patient (4%) had lesions due to oxaliplatin (20 lesions), four patients (17%) had intraductal papillary neoplasm of bile duct (BT-IPNB), in one case degenerated, one patient (4%) had melanoma of intrahepatic bile ducts, three patients (13%) had cystadenoma (with one case of cystadenocarcinoma), one patient (4%) had bile ducts lymphoma and one patient (4%) had biliary adenoma. 13 patients (56%) had also undergone CT study (10 patients with biliary metastases, one with lesions to oxaliplatin, one with melanoma, and one with degenerated IPNB) and eight patients (35%) had also undergone US and CEUS study (five patients with biliary metastases, one with oxaliplatin injury, one with melanoma and one with degenerated IPNB).

Imaging features

The size of the lesions, for intraductal and intrahepatic tumours, ranged between 4 and 100 mm. With reference to the anatomical site, in 5/23 patients (22%) the lesion was intraductal, in 14/23 patients (61%) the lesion was periductal (all defined as a single lesion), and in 4/23 patients (17%) the lesion was intrahepatic. With reference to the structure, 16/23 (70%) patients had solid lesions, 5/23 (22%) cystic lesions and 2/23 (9%) complex cystic lesions.

No significant difference was found in the diameters of each measurable intrahepatic lesion on the various CEUS, CT and MR images and among MR sequences (p value > 0.05).

Among the cystic lesions, the lesion was simple in five cases (three patients with BT-IPNB and two with cystadenoma). It showed a signal intensity on T_1 W images and T_2 W images similar to that of the gallbladder. The lesion showed a restricted diffusion from b0 s/mm^2 to b800 s/mm^2 and a mean ADC value of 1.59×10^{-3} mm^2 s^{-1}. In two patients with complex cystic lesion (one with cystadenocarcinoma and another with degenerated IPNB), the cystic component of the lesion was combined with a solid one that was heterogeneously hypointense on T_1 W flash in-out phase images and in pre-contrast VIBE T_1 W

images, and hyperintense on T_2 W imaging. This solid portion showed a restricted diffusion from b0 s mm^{-2} to b800 s mm^{-2} and a mean ADC value of 1.29 × 10^{-3} mm^2 s^{-1}. During the contrast study on CT, MR and US, the solid component showed heterogeneous contrast enhancement, with wash-out during the delayed phase.

Among the solid lesions, in two patients these were intrahepatic (lesions to oxaliplatin and biliary adenoma), with signal hypointense on T_1 W flash in-out phase images and in pre-contrast VIBE T_1 W images, hyperintense on T_2 W imaging; diffusion was restricted from b0 s mm^{-2} to b800 s mm^{-2} and a mean ADC value of 1.93 × 10^{-3} mm^{2}s^{-1}. During contrast study the lesions to oxaliplatin showed heterogeneous contrast enhancement, many of these showed wash-in on arterial phase, isointense signal on portal and late phase and peripheral hyperintense rim during hepatospecific phase on MR study. The remaining periductal solid lesions (12 patients with biliary metastases and the patient with lymphoma) showed hypointense signal on T_1 W flash in-out phase images and in pre-contrast VIBE T_1 W images, hyperintense signal on T_2 W imaging. The diffusion was restricted from b0 s mm^{-2} to b800 s mm^{-2} and a mean ADC value of 1.31 × 10^{-3} mm^{2}s^{-1}. During the contrast-enhanced study, the lesion showed a progressive contrast enhancement. We found no significant difference in signal and contrast enhancement among all periductal metastases on the T_1 W flash 2d in-out phase, on the HASTE T_2 W, portal and hepatobiliary-phase VIBE T_1 W images on MR images and on CEUS and CT images (p value > 0.05).

Peribiliary melanoma showed hyperintense signal on T_1 W flash in-out phase images and in pre-contrast VIBE T_1 W images and hyperintense signal on T_2 W imaging. The diffusion was restricted from b0 s mm^{-2} to b800 s mm^{-2} and ADC value of 1.42 × 10^{-3} mm^2 s^{-1}. During the contrast study, the lesion showed a progressive contrast enhancement.

DISCUSSION

The biliary tract cancers, CCC excluded, are rare entities, including benign, borderline and malignant lesions. They can be divided into cystic and solid lesions.[1] Imaging plays a crucial role. US and CT are often employed in diagnostic work-up of the biliary tract abnormalities. MRI, thanks to high contrast resolution, technological evolution and use of contrast agents eliminated by the biliary system, is the method of choice for biliary tract.[7,8]

Among the benign biliary abnormalities, a new entity, whose impact is still uncertain, is represented by lesions secondary to the use of oxaliplatin.[10] Oxaliplatin is one of chemotherapy administered to patients with metastatic colorectal cancer, and it is responsible for damage of the liver sinusoids.[11] The damage can lead to the development of solid lesions, whose differential diagnosis with metastatic lesions remains a challenge (Figure 1). In our study, a single patient had twenty lesions, histologically proven, due the use of oxaliplatin. On US, the lesions were heterogeneously isoechoic or hypoechoic, while on CT, during the portal phase, several lesions were isodense while other lesions were hypodense.[12] MRI with hepato-specific contrast medium is often the method that best enables for assessing benign lesion. In our patient, we detected some lesions on morphological T_2 W and T_1 W sequences, and these showed hyperintense signal on T_2 W and hypointense signal on T_1 W. During the arterial phase, we found hypervascular lesions that in the portal and late phase, became isointense or hypointense. During the hepatobiliary phase, the lesions accumulated the contrast medium, resulting isointense with a hyperintense rim or hyperintense (Figure 2). However, it is also reported the possibility of a hypodense

Figure 1. 42-year-old male with history of rectal cancer. Oxaliplatin-induced lesions. US (a) shows solid, isoechoic to hypoechoic lesions (arrow). In (b, c) CT scan on portal phase of dynamic study: the lesion is hyperdense or isodense with hyperdense peripheral rim (arrow). Liver lesions appear hyperintense (arrow) on T_2 W MR images (d) hypointense (arrow) on T_1 W MR images (e) out-of-phase sequence and (f) in-of-phase).

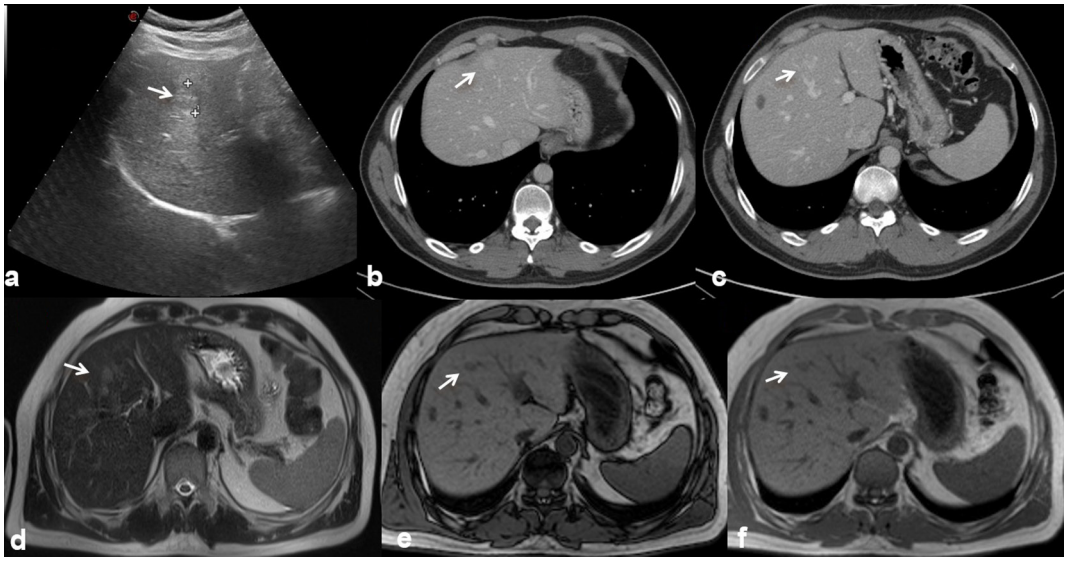

Figure 2. The same patient of Figure 1. DWI (a, b50; b b800; c, ADC map) shows a restricted diffusivity of the lesions (arrow), with mean ADC value of 1.93 × 10–3 mm^2 s^{-1}. The lesion is hyperintense (arrow) on arterial-phase images (d VIBE T1-W FS sequence), hyperintense (arrow) on portal-phase MR images (e) isointense with hyperintense peripheral rim (arrow) on hepatospecific phase images (f).

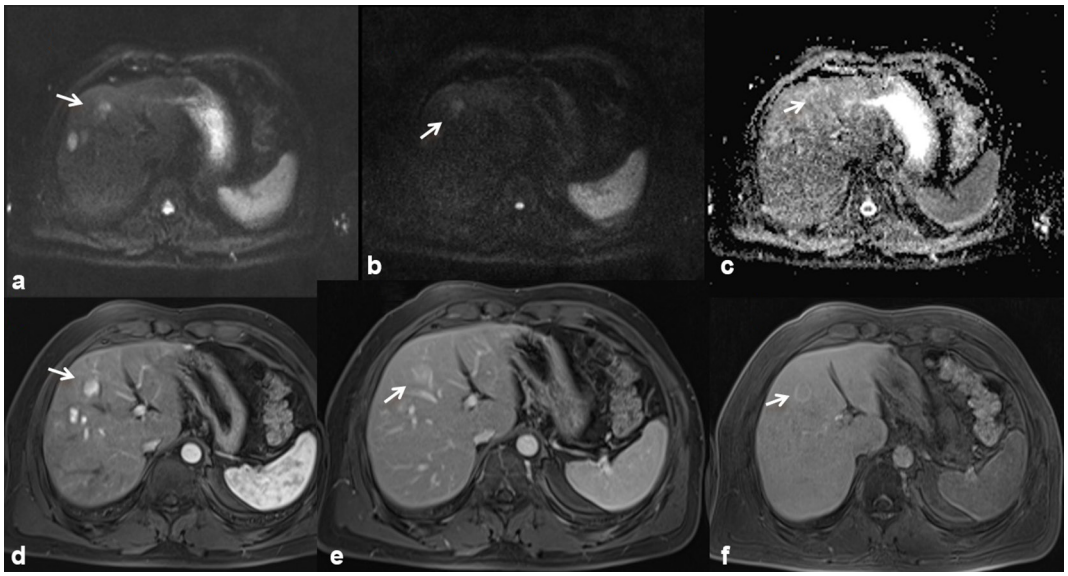

appearance in the hepatobiliary phase, mimicking metastasis.[13] The diffusion was restricted from b0 s mm^{-2} to b800 s mm^{-2} and a mean ADC value of 1.93 × 10–3 mm^2 s^{-1}. Many nodules were identified only after the administration of contrast medium. In our series, MR study, thanks to the possibility to use a hepatospecific contrast medium, allowed a better characterization oxaliplatin lesion as benign, compared with US or CT. In fact, a hyperintense or isointense signal on hepatobiliary phase is typical of benign lesions. However, the clinical history, a chemotherapy regimen based on oxaliplatin, the absence of lesions before the beginning of the treatment, the multiplicity of the lesions and the stability in time should be elements for a proper diagnosis. We suggested use of MRI with EOB to follow-up patients with oxaliplatin lesions.

Figure 3. 45-year-old female with epigastric pain. Cystadenoma. US (a) detects a perigastric hypoechoic mass (arrow). Operative specimen of cystadenoma (b and c).

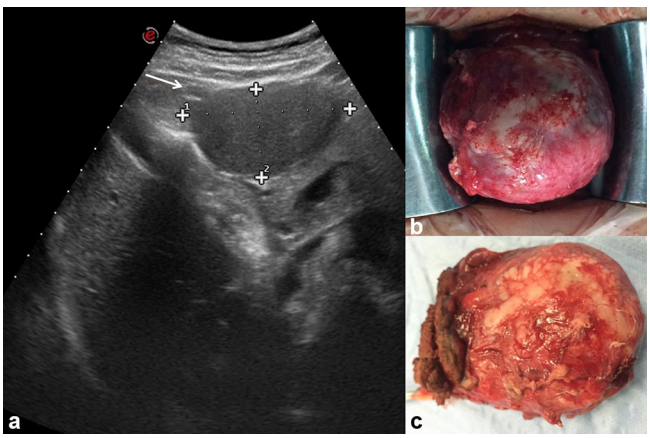

The most frequent cystic biliary lesion is cystadenoma.[14] Cystadenoma (Figure 3) is a rare tumour, with an incidence of approximately 5% of all biliary cystic lesions.[14,15] The aetiology is unknown. The tumour most often originates from the intrahepatic bile ducts;[15] rarely, it has been reported in the extrahepatic bile ducts and gallbladder.[15] Females are more frequently affected than males and the mean age in which the lesion is discovered is around 45 years.[16] Liver function tests are abnormal, with an increased level of bilirubin and transaminases. An increased serum level of CA 19–9 and CEA has also been reported.[14–16] Elevated levels of CA 19–9 and CEA have also been demonstrated within the cyst fluid.[17] Although cystadenoma is a benign lesion, it could have a malignant transformation into a cystadenocarcinoma.[18] It has been reported a case of sarcomatous evolution.[19] In our series we found three patients with cystadenoma (all proven histologically), with one case of transformation in cystadenocarcinoma. On US the lesion appears as a large expansive hypoechoic mass. On CT examination, the area is hypodense; while in MRI, the intracystic signal on T_1 and T_2 W is reported as variable, in relation to the concentration of protein and heme degradation products, most commonly low signal on T_1 W and high on T_2 W, as all the cystic lesions.[20] In our series, cystadenomas appeared as hypointense on T_1 W and lower hyperintense than gallbladder on T_2 W images (Figure 4). The presence of mural contrast enhancement is not specific (Figure 5). The mural nodule is an element that must be readily recognized to suspect transformation in cystadenocarcinoma[20] (Figure 6). The differential diagnosis between cystadenoma and cystadenocarcinoma is not easy. Therefore, surgical resection is recommended for all cystic lesions suspicious for cystadenoma.[20]

Recently, the term of intraductal papillary neoplasm of the biliary tract (BT-IPMN) has been proposed to describe a tumour

Figure 4. The same patient of Figure 3. MRI demonstrates a complex lesion with proteinaceous content. The lesion is iso-hyperintense (arrow) on T_2 W (HASTE, (a, coronal view; b, axial view) and on T_1 W (c, in-of-phase and d, out-of-phase axial image). HASTE, half-Fourier acquisition single-shot turbo spin-echo.

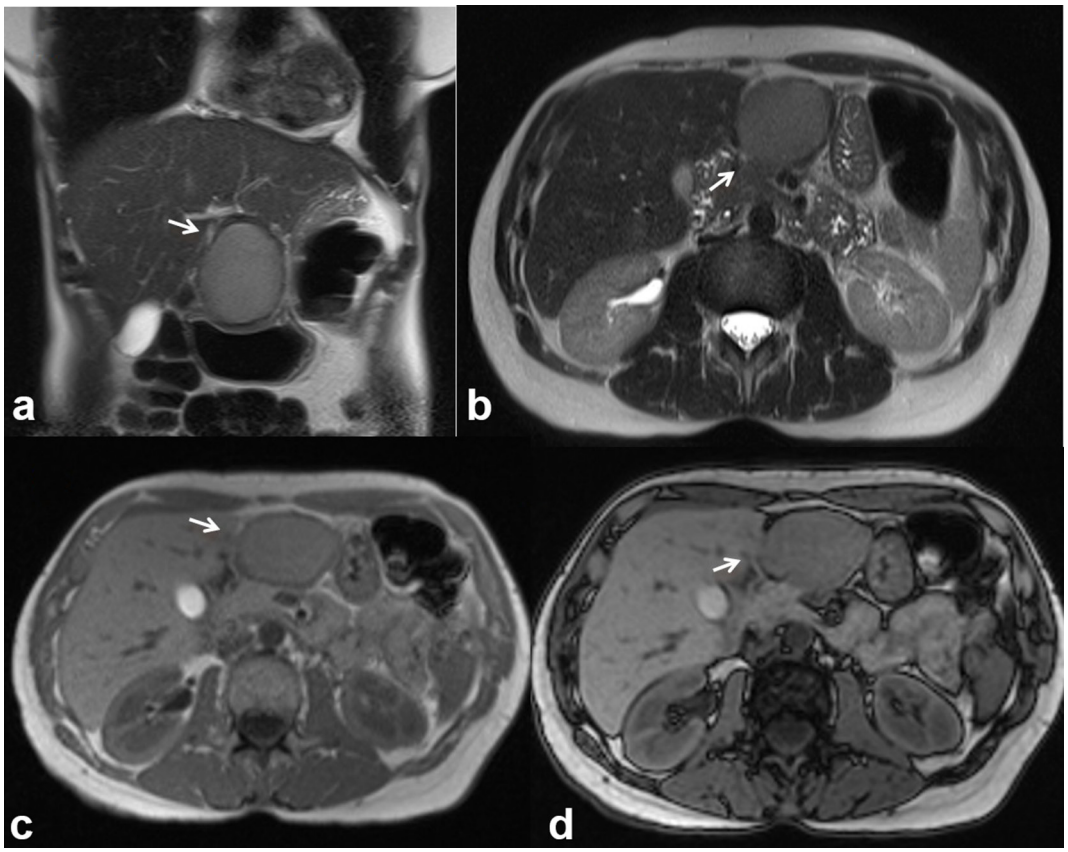

of the biliary tract, characterized by the presence of intraluminal papillary lesions, with a fibrovascular core inside of dilated bile ducts.[21] The neoplastic cells produce an excess of mucin.[21] Histologically, the BT-IPMN is defined as a papillary mucinous lesion, which originates from biliary epithelium, characterized by a solitary or widespread growth. Four histological subtypes are known (gastric, intestinal, biliopancreatic and oncocytic).[22] It is a rare entity, which can involve both the intrahepatic and

Figure 5. The same patient of Figures 3 and 4. Arterial (a, VIBE FS T_1 W, axial plane) and portal-phase images (b, VIBE FS T_1 W, axial image;c, coronal image) demonstrate the mural enhancement (arrow). Diffusion sequence images (d, b50; e, b800; f, ADC map) show a restricted diffusivity with an ADC value of 1.64×10^{-3} mm^2s^{-1}.

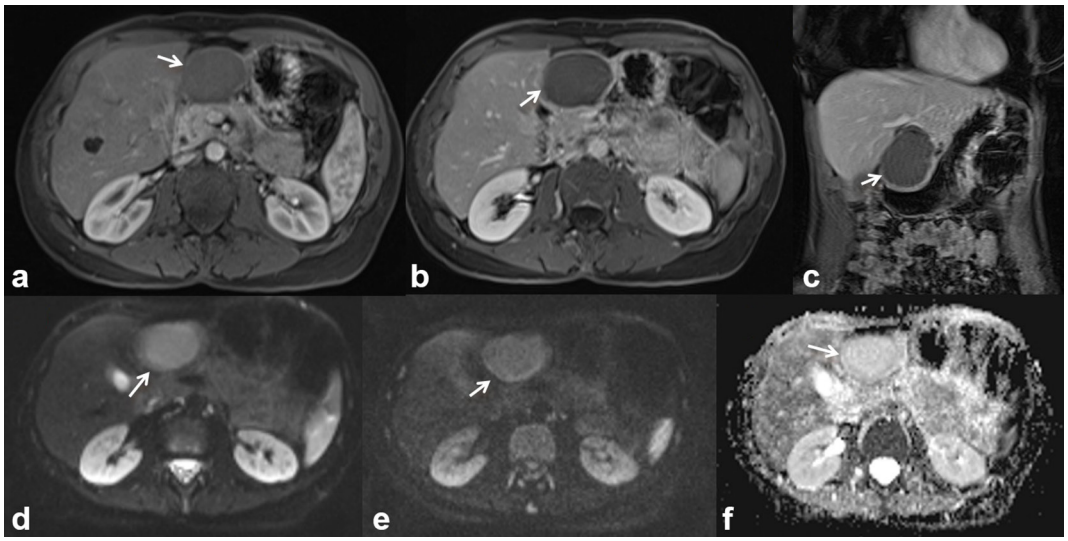

Figure 6. 50-year-old female. Cystadenocarcinoma. Cystic mass with a solid, enhancing mural nodule (arrow). The mural nodule appears hyperintense (arrow) on T_2 W images (a, HASTE T_2 W coronal view; b, single-shot cholangiographic image), hyperintense (arrow) on hepatospecific phase on contrast study (c, VIBE T_1 W FS image coronal plane), hypeintense on contrast-enhanced arterial-phase axial image (d, VIBE T_1 W FS axial plane), contrast-enhanced portal-phase axial image (e) and contrast-enhanced hepatobiliary phase axial image (f). HASTE, half-Fourier acquisition single-shot turbo spin-echo.

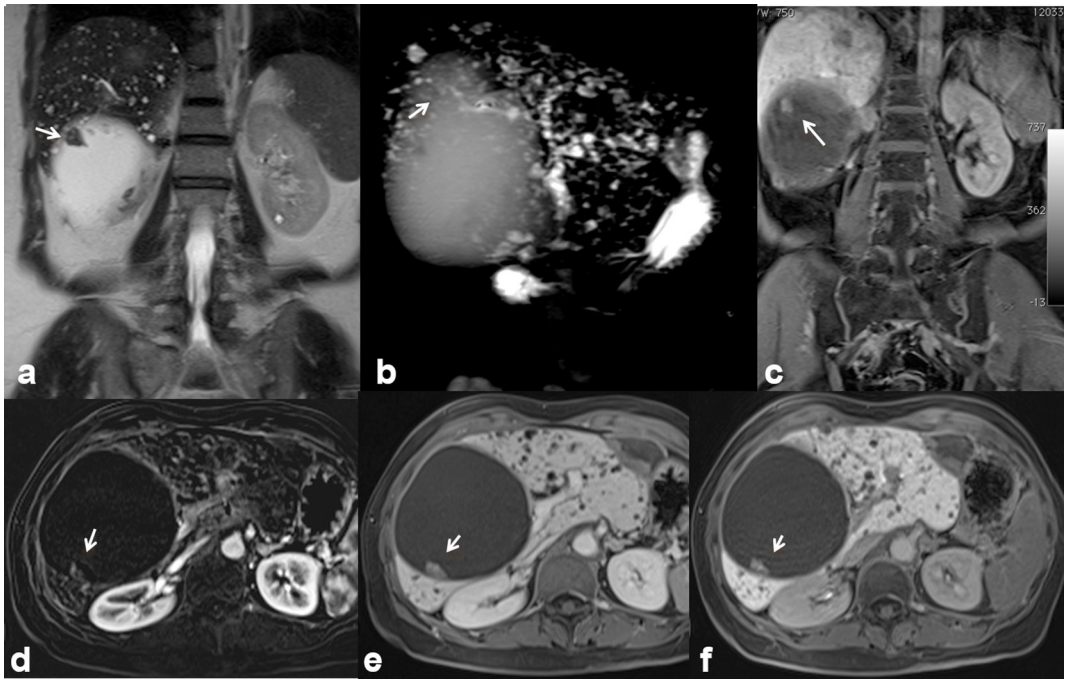

extrahepatic bile ducts,[21,22] representing the precursor of tubular adenocarcinoma or mucinous carcinoma.[22] BT-IPMN shows some clinical, pathological and radiological features similar to pancreatic IPMN (P-IPMN), with a significant difference in terms of potential degeneration. The probability of a malignant degeneration for BT-IPMN is higher (64–89%) compared with P-IPMN (23–30%), being correlated with the prevalence of intestinal and biliopancreatic subtypes, which have a greater biological aggressiveness.[21–23] The features that should be considered for a correct diagnosis is the finding of mucobilia, dilated ducts, shape, enhancement and the metabolic activity of mural nodules. The dilatation of the bile ducts upstream to the lesion is a frequently observed sign in the BT-IPMN,[24] although this type of lesion is often associated also with an expansion downstream of the biliary tract. There are described cases in which the entire biliary tree is dilated, as result of excessive production of mucin.[24] The majority of malignant BT-IPMN forms have wall nodules with contrast enhancement or solid component that infiltrates the adjacent liver parenchyma (Figure 5).[24] The BT-IPMN may appear as a small lesion or as a focal thickening of the wall up to the lesion.[25] However, more often the tumour is small and not visible directly at imaging and therefore indirect signs have to be searched for.[21–25] US is the first technique used in a hepatic disease. Although it is possible to directly identify the lesion with ultrasounds, when it is of considerable size, more frequently indirect signs are displayed, such as the mucin and the districtual dilatation of the biliary tract.[25] The papillary tumours can be identified both by CT and MRI. When the lesion is small it is more often unrecognized and, therefore, even in these cases it is necessary to look for indirect signs such as dilation of the biliary tract and the presence of mucin. On the CT and MR images, it is hard to identify the presence of mucin since it shows the same density and signal intensity of the bile. Therefore, also MR-cholangiography does not allow the characterization of mucin.[25] Gd-EOB-DTPA allows an indirect visualization of the mucin, because the bile duct in which this substance is present will appear in hepatobiliary phase as a devoid of signal. Large lesions, such as wall nodules, or the solid component that infiltrates the liver parenchyma and that presenting a contrast enhancement after intravenous contrast medium are indices of malignancy.[25]

The treatment of choice, given the precancerous nature of the lesion, is liver resection.[23–25] In the examined cases (all proven histologically), no patient with BT-IPMN was evaluated with US or CT, while all of them were evaluated with MRI. On T_2 W sequences, the lesions appeared as expansive, hyperintense, with a continuation of the bile ducts, while on T_1 W images showed hypointense signal. After contrast medium injection there was no evidence of contrast enhancement (Figure 7). The diffusion was restricted from b0 s mm^{-2} to b800 s mm^{-2} with an ADC value of 1.42 × 10^{-3} mm^2 s^{-1}. The only patient with degenerated BT-IPMN was studied with all imaging modalities. On US the solid component appeared heterogeneously iso-hyperechoic with contrast-enhancement during CEUS (Figure 8). On CT the solid component, infiltrating the liver parenchyma, showed an inhomogeneous contrast enhancement, predominantly peripheral during the arterial phase, with centripetal

Figure 7. 53-year-old female. BT-IPMN. The lesion's signal intensity is similar to that of the biliary ducts on the T_2 W images (a, HASTE), arrow shows continuity with biliary tree. In (b) (in-of-phase T_1 W in axial plane) and (c) (out-of-phase T_1 W FS in axial) the lesion is hypointense (arrow); (c, maximum intensity projection). Diffusion sequence images (d, b800; e, ADC map) show a restricted diffusivity (arrow) with an ADC value of 1.42×10^{-3} mm^2s^{-1}. T_1 W VIBE FS portal-phase image (f) shows a fluid, non-enhancing lesion (arrow). HASTE, half-Fourier acquisition single-shot turbo spin-echo.

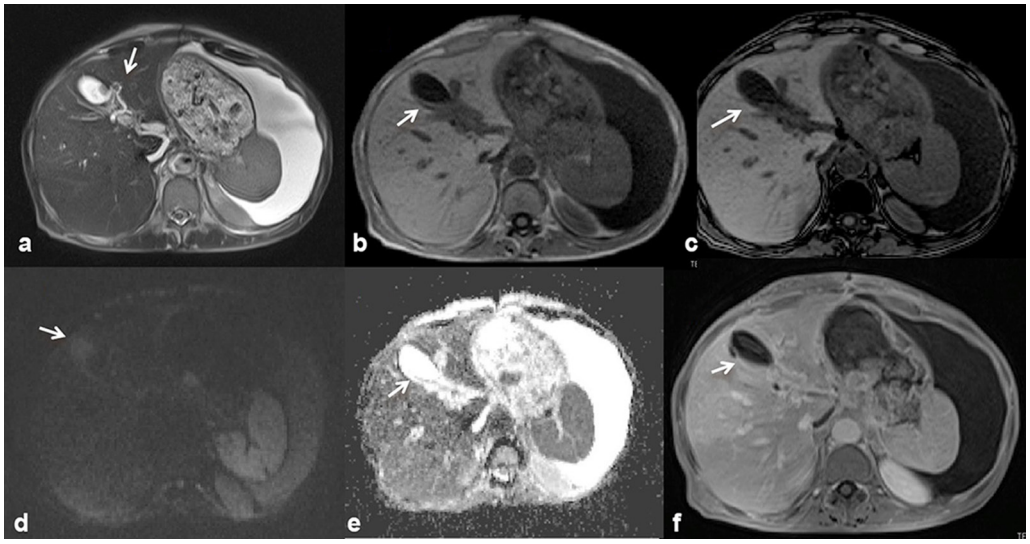

trends in the portal and late phases. On MR the solid portion appeared with a hypointense signal on T_1 W and hyperintense on T_2 W sequences (Figure 9). After contrast medium it showed an inhomogeneous contrast enhancement, predominantly peripheral during arterial phase, with centripetal trends in the portal and late phases (Figure 10). The diffusion was restricted from b0 smm^{-2} to b800 s mm^{-2} with an ADC value of 1.29×10^{-3} mm^2 s^{-1}.

Figure 8. 74-year-old male. Degenerated BT-IPMN. Complex, bilobated lesion with a solid and cystic component. On US, the solid component (arrow) appears heterogeneously iso-hyperechoic with contrast-enhancement during CEUS (a–h).

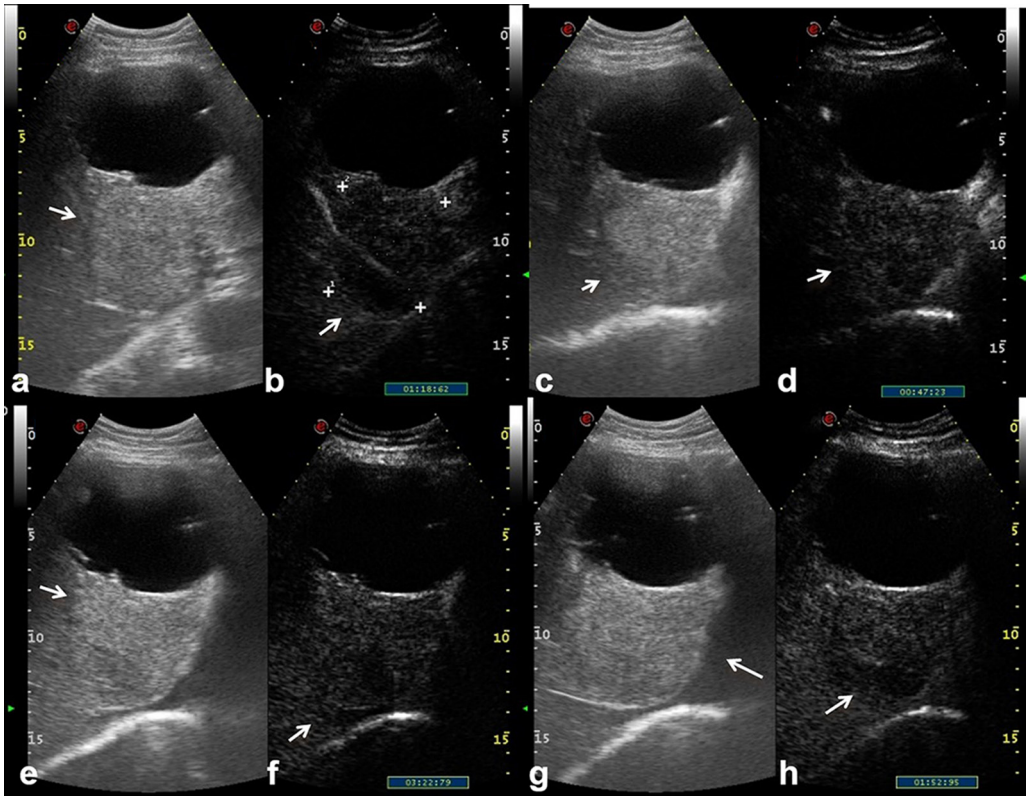

Figure 9. The same patient of Figure 8. T_2 W, HASTE images (a, axial plane; b, coronal plane) show the continuity with a biliary duct, while the solid component appears hyperintense on T_2 W (a, b) and hypointense (arrow) on T_1 W (c), in-of-phase T_1 W and (d), out-of-phase T_1 W. HASTE, half-Fourier acquisition single-shot turbo spin-echo.

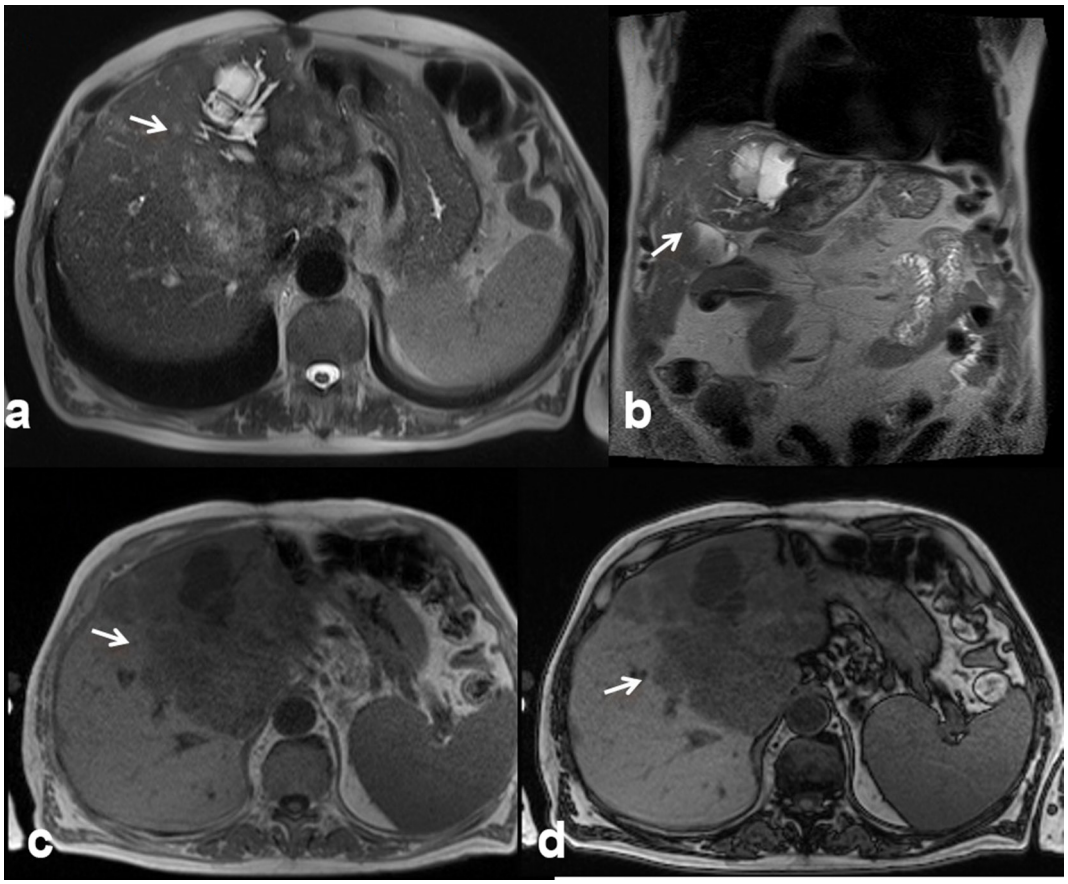

Figure 10. The same patient of Figures 8 and 9. Restricted diffusivity on DW images (a, b50; b, b800; c, ADC map) with an ADC value of 1.29×10^{-3} mm^2s^{-1}. After contrast medium it showed an inhomogeneous contrast enhancement, predominantly peripheral (arrow) during arterial phase (d, VIBE T_1 W FS in axial plane), with centripetal trends in the portal (e) and late phase (f). In (g) axial CT scan during portal phase of contrast study, the solid component appears iso-hyperdense.

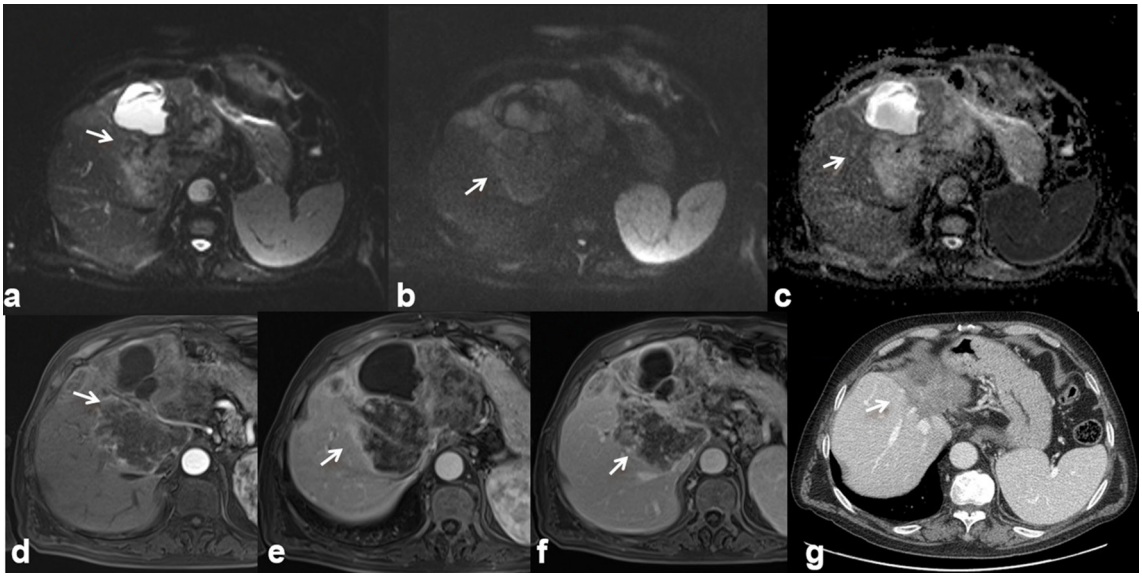

Figure 11. 46-year-old male. Biliary adenoma. Single, subcapsular solid lesion, appearing as hyperintense (arrow) in T2-W images (a, HASTE) and hypointense (arrow) in T_1 W images (b, out-of- phase T_1 W; c, in-of-phase T_1 W and d, pre-contrast FS VIBE T1-W). HASTE, half-Fourier acquisition single-shot turbo spin-echo.

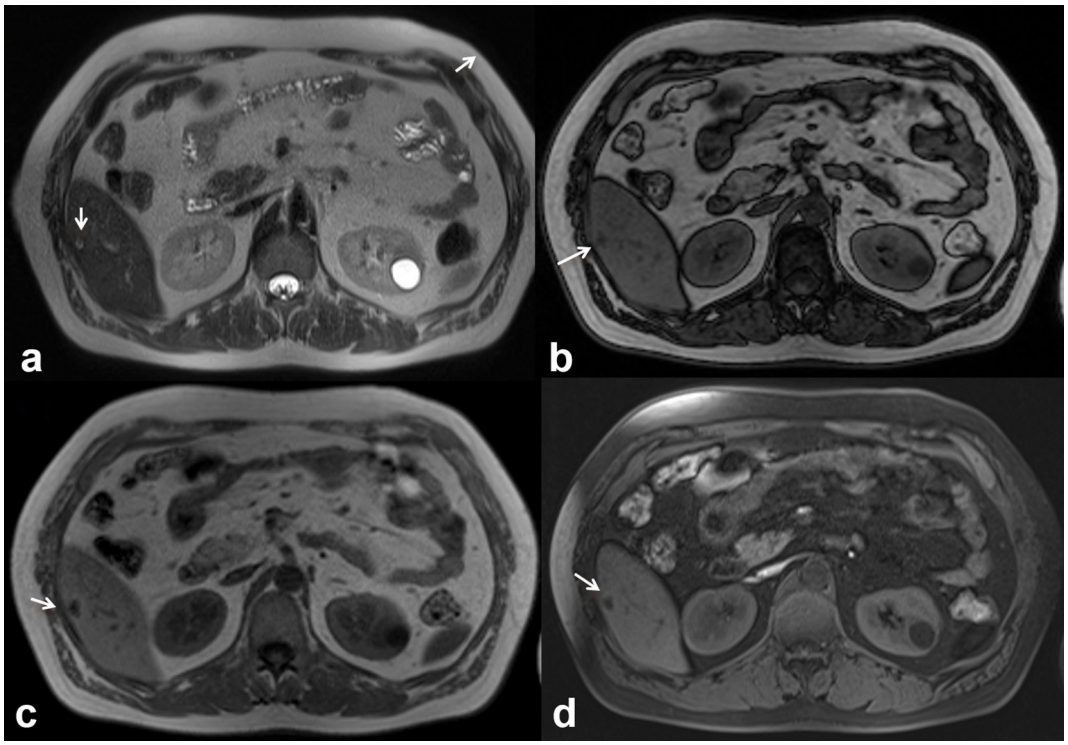

Intrahepatic bile duct adenoma (BDA) is a rare tumour that originates from the epithelium of the bile ducts with an incidence of 1.3%.[26] It is described as a well-defined, non-capsulated, non-cystic and small (<2 cm) subcapsular lesion (Figure 11). Histologically, the BDA is characterized by inflammatory cells and fibrosis around the bile ducts, as a response to an insult, often associated with chronic disease. In MRI, the lesion shows variable signal on T_1 W sequences and is usually hyperintense on T_2 W. During the dynamic study, BDA is hypervascular with loss or persistence of the contrast in relation to the degree of fibrosis.[27] The possibility of a malignant degeneration is extremely rare and, therefore, further studies are required for anappropriate therapeutic management of the lesion.[26–28] In our series the only BDA, proven histologically, appeared as a subcapsular lesion, with a low signal on T_1 W, high signal on T_2 W, hypervascular during arterial phase of contrast study with persistence of the contrast during portal and late phases.

The most common solid malignant tumour affecting the bile ducts, after CCC is metastasis. The cancers that most frequently metastasize to the biliary tract are those of the gastrointestinal tract (such as the colorectum, stomach and pancreas), breast, lung, melanoma, kidney and lymphoma[29] (Figure 12). Imaging does not allow a correct differential diagnosis from cholangiocarcinoma because there is an overlap of the radiological features and metastasis can mimic all three aspects of CCC.[29] Although positron emission tomography is a sensitive technique for the detection of peribiliary tumours, it is not specific in the differential diagnosis of CCC.[30] The anatomical site more often involved from metastasis is the common hepatic duct, both for the presence of newly formed tissue and for the involvement of the hepatoduodenal ligament lymph-nodes.[30,31] CT and MRI are the methods that allow an appropriate assessment of peribiliary metastases. In our series we found no significant difference in signal and contrast enhancement among all periductal metastases on the T_1 W, on T_2 W, arterial, portal, late and hepatobiliary-phase on MR images, on portal-phase CEUS images, and on portal-phase CT images. In our series the lesions were not recognized at US. Additionally, at CT imaging the lesions were not identified until after the review of images based on MR findings. The lesions showed hypointense signal on T_1 W, hyperintense signal on T_2 w. The diffusion was restricted from b0 smm^{-2} to b800 smm^{-2} with a mean ADC value of 1.28×10^{-3} mm^2s^{-1}. During contrast study, the lesion showed a progressive contrast enhanced (both MR than CT studies), according to a previous study.[32]

Biliary melanoma can be either primary or metastatic. Until now, at the best of our knowledge, there are 10 cases of known primary peribiliary melanoma.[33–36] Usually, the biliary melanoma has a soft intraluminal polyp with a biliary dilation.[34] The more often involved location is the common hepatic duct, although it is also described in intrahepatic ducts (Figure 13) or gallbladder.[33,34] US identifies indirect signs, such as a biliary dilatation, and only in case of large tumours can highlight the jutting lesion in the biliary lumen.[36] MRI identifies the lesion as a mass of soft tissue, with variable signal intensity on T_1 W, in relation to the paramagnetic effect of melanin and high signal on T_2 W sequence.[36] After contrast injection both in CT and MRI a progressive and gradual contrast enhancement may appear.[36] In

Figure 12. 56-year-old female. Pancreatic cancer with peribiliary liver metastases. The metastatic tissue is hyperintense (arrow) on T2-W HASTE images (a) and hypointense on T_1 W images (b, in-of-phase T_1 W and c out-of-phase T_1 W). Diffusivity is restricted on DW images (d, b800;e, ADC map) with a mean ADC value of 1.28×10^{-3} mm^2 s^{-1}. Vascularized tissue (arrow) (f, arterial and g, portal-phase T_1 W VIBE images).

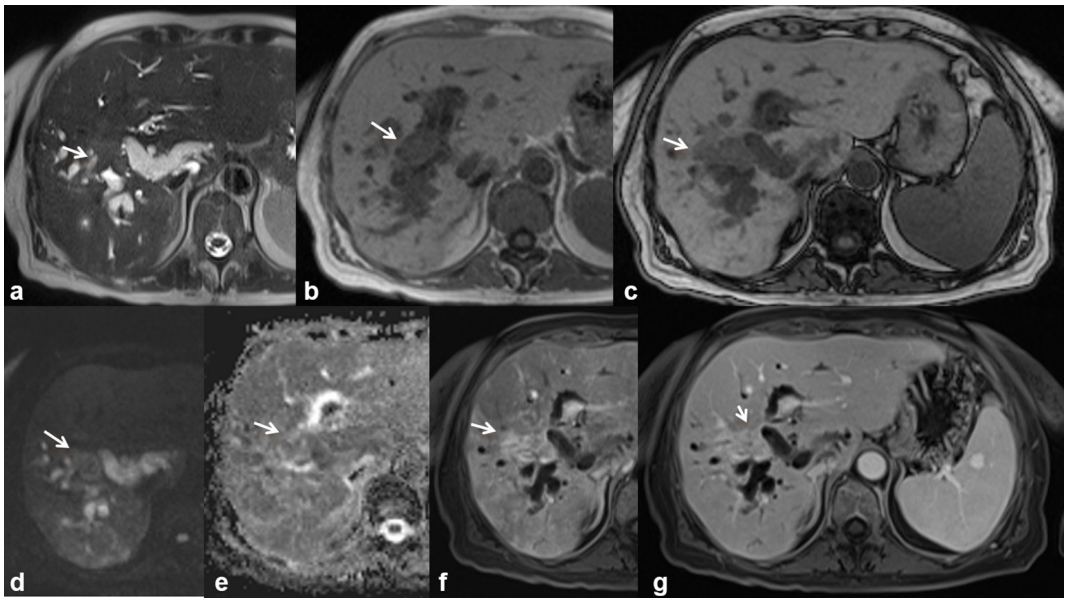

Figure 13. 37-year-old male. Primary peribiliary melanoma. Hyperintense peribiliary tissue (arrow) visible on T_2 W images (HASTE coronal (a) and axial (b) view) with distrectual dilation of the biliary ducts. Restricted diffusivity on DW images (c, b50; d, b800; e, ADC map) with an ADC value of 1.42×10^{-3} mm^2s^{-1}. Hyperintense (arrow) appearance on T_1 W (f, out-of-phase T_1 W and g, in-of-phase T_1 W). The lesion is hyperintense (arrow) on contrast-enhanced arterial phase (h, T_1 W VIBE FS), isointense on contrast-enhanced portal-phase images (i) and hypointense on hepato-specific phase images (j), with a hypointense appearance of the dilated biliary ducts. In (k) operative specimen of hepatic primitive melanoma (arrows).

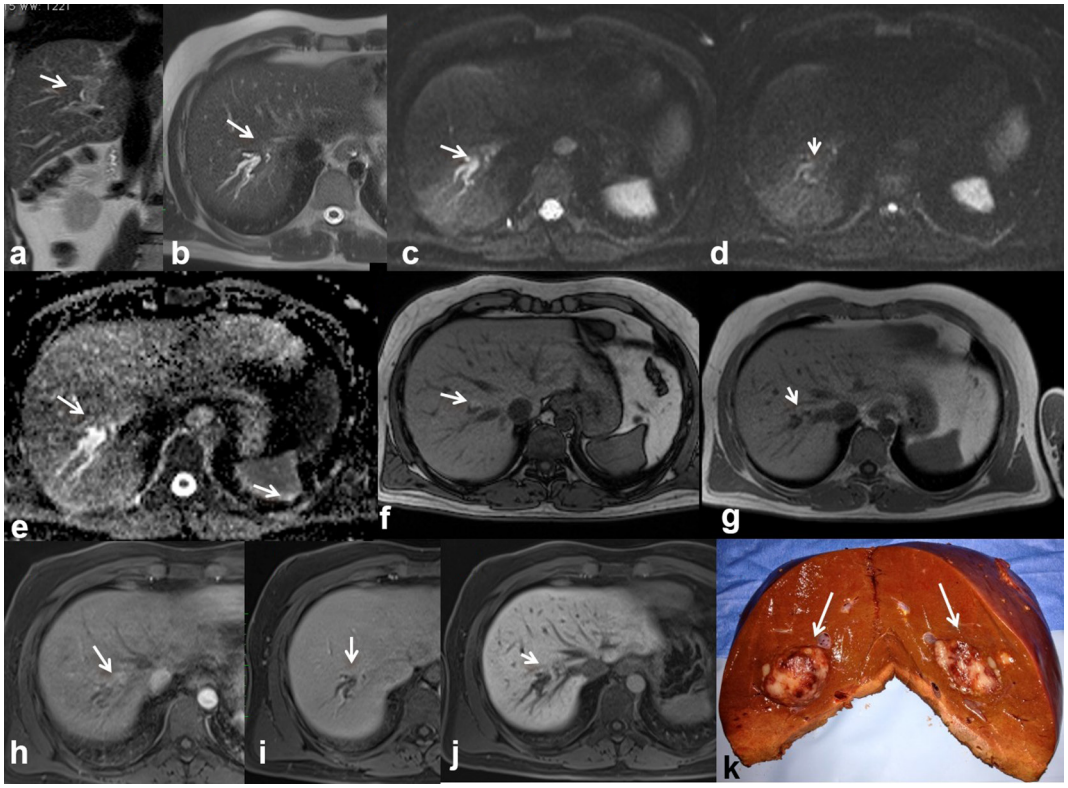

Figure 14. 39-year-old male. Primary lymphoma. Solid tissue penetrating from the liver hilum around the right and left intrahepatic bile ducts. The tumour tissue is hyperintense (arrow) on T_2 W images (a, HASTE in axial plane) and hypointense (arrow) on T_1 W images (b, out-of-phase T_1 W). The lesion shows a contrast enhanced (arrow) on portal phase of contrast study (c, VIBE T_1 W FS in axial plane).

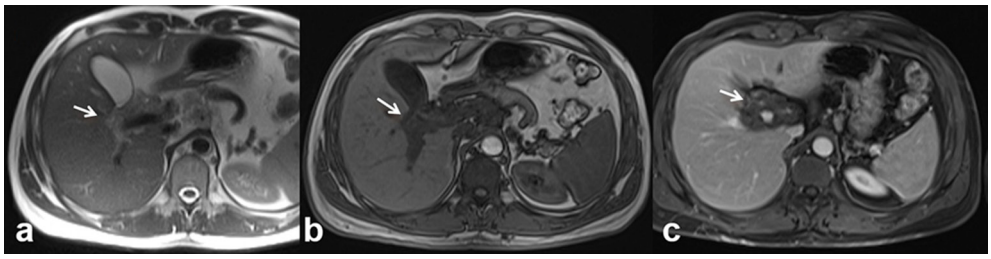

our series, as already reported in the literature,[33–36] US and CT identified only the indirect signs, such as biliary dilatation. MRI identified the lesion as hyperintense on T_1 W, hyperintense on T_2 W, with restricted diffusion and with a ADC value of 1.42×10^{-3} mm^2s^{-1}. During contrast study, the lesion showed a progressive contrast enhancement.

B-cell lymphoma is the most common form of lymphoma that affects the bile ducts.[28] The tumour may involve both branches of the bile ducts and the common hepatic duct, resulting in a reduction of caliber, but not necessarily a complete ductal obstruction as CCC (Figure 7). The tumour can also spread through the peribiliary intrahepatic ducts (Figure 14). On US, the lesion may be visible as a peribiliary hypoechoic tissues or increase of periportal spaces. During contrast studies, both CT and MRI, the tumour shows a progressive and slow contrast enhancement. T_1 W shows the lesion as moderately hypointense, while on T_2 W it has a moderately high signal, higher than CCC.[37] In our series we performed only MRI, and the lesion appeared hypointense on T_1 W, hyperintense on T_2 W imaging, with restricted diffusion and with a ADC value of 1.34×10^{-3} mm^2s^{-1}. During contrast study, the lesion showed a progressive contrast enhancement.

CONCLUSION

Biliary tract tumours can vary significantly in location, growth pattern and histologic subtype. These tumours can have a wide spectrum of radiologic appearances and uncommon lesions generally represent a diagnostic challenge for radiologists, because the radiological features frequently overlap. Although US is the primary modality employed in the evaluation of biliary tract, it is less accurate in the assessment of tumour spread and tumour resectability compared with CT and MRI. Given that this information is crucial for tumour staging and treatment planning, MRI is the technique to choose for patients with suspected biliary tumours.

ACKNOWLEDGMENTS

The authors are grateful to Maria Bruno, Laura Galeani, Rita Guarino, Alessandra Trocino and Assunta Zazzaro for the collaboration.

REFERENCES

1. Pedrassa BC, da Rocha EL, Kierszenbaum ML, Bormann RL, Torres LR, D'Ippolito G. Uncommon hepatic tumors: iconographic essay - Part 1. *Radiol Bras* 2014; **47**: 310–6. doi: https://doi.org/10.1590/0100-3984.2013.1760
2. Mittal PK, Moreno CC, Kalb B, Mittal A, Camacho JC, Maddu K, et al. Primary biliary tract malignancies: MRI spectrum and mimics with histopathological correlation. *Abdom Imaging* 2015; **40**: 1520–57. doi: https://doi.org/10.1007/s00261-014-0300-0
3. Corona-Villalobos CP, Pawlik TM, Kamel IR. Imaging of the patient with a biliary tract or primary liver tumor. *Surg Oncol Clin N Am* 2014; **23**: 189–206. doi: https://doi.org/10.1016/j.soc.2013.10.002
4. Corvino A, Catalano O, Setola SV, Sandomenico F, Corvino F, Petrillo A. Contrast-enhanced ultrasound in the characterization of complex cystic focal liver lesions. *Ultrasound Med Biol* 2015; **41**: 1301–10. doi: https://doi.org/10.1016/j.ultrasmedbio.2014.12.667
5. Granata V, de Lutio di Castelguidone E, Fusco R, Catalano O, Piccirillo M, Palaia R, et al. Irreversible electroporation of hepatocellular carcinoma: preliminary report on the diagnostic accuracy of magnetic resonance, computer tomography, and contrast-enhanced ultrasound in evaluation of the ablated area. *Radiol Med* 2016; **121**: 122–31. doi: https://doi.org/10.1007/s11547-015-0582-5
6. Graziani R, Mautone S, Ambrosetti MC, Manfredi R, Re TJ, Calculli L, et al. Autoimmune pancreatitis: multidetector-row computed tomography (MDCT) and magnetic resonance (MR) findings in the Italian experience. *Radiol Med* 2014; **119**: 558–71. doi: https://doi.org/10.1007/s11547-013-0373-9
7. Bartolotta TV, Taibbi A, Midiri M, La Grutta L, De Maria M, Lagalla R. Characterisation of focal liver lesions undetermined at grey-scale US: contrast-enhanced US versus 64-row MDCT and MRI with liver-specific contrast agent. *Radiol Med* 2010; **115**: 714–31. doi: https://doi.org/10.1007/s11547-010-0506-3
8. Palmucci S, Mauro LA, La Scola S, Incarbone S, Bonanno G, Milone P, et al. Magnetic resonance cholangiopancreatography and contrast-enhanced magnetic resonance cholangiopancreatography versus endoscopic ultrasonography in the diagnosis of

extrahepatic biliary pathology. *Radiol Med* 2010; **115**: 732–46. doi: https://doi.org/10.1007/s11547-010-0526-z
9. Granata V, Catalano O, Fusco R, Tatangelo F, Rega D, Nasti G, et al. The target sign in colorectal liver metastases: an atypical Gd-EOB-DTPA "uptake" on the hepatobiliary phase of MR imaging. *Abdom Imaging* 2015; **40**: 2364–71. doi: https://doi.org/10.1007/s00261-015-0488-7
10. Uchino K, Fujisawa M, Watanabe T, Endo Y, Nobuhisa T, Matsumoto Y, et al. Oxaliplatin-induced liver injury mimicking metastatic tumor on images: a case report. *Jpn J Clin Oncol* 2013; **43**: 1034–8. doi: https://doi.org/10.1093/jjco/hyt113
11. Arakawa Y, Shimada M, Utsunomya T, Imura S, Morine Y, Ikemoto T, et al. Oxaliplatin-related sinusoidal obstruction syndrome mimicking metastatic liver tumors. *Hepatol Res* 2013; **43**: 685–9. doi: https://doi.org/10.1111/j.1872-034X.2012.01114.x
12. Alexandrino H, Oliveira D, Cipriano MA, Ferreira L, Tralhão JG, Castro E Sousa F. Oxaliplatin toxicity presenting as a liver nodule - case report. *BMC Cancer* 2015; **15**: 247. doi: https://doi.org/10.1186/s12885-015-1247-4
13. Shin NY, Kim MJ, Lim JS, Park MS, Chung YE, Choi JY, et al. Accuracy of gadoxetic acid-enhanced magnetic resonance imaging for the diagnosis of sinusoidal obstruction syndrome in patients with chemotherapy-treated colorectal liver metastases. *Eur Radiol* 2012; **22**: 864–71. doi: https://doi.org/10.1007/s00330-011-2333-x
14. Soochan D, Keough V, Wanless I, Molinari M. Intra and extra-hepatic cystadenoma of the biliary duct. review of literature and radiological and pathological characteristics of a very rare case. *BMJ Case Rep* Apr 2012. Epub ahead of print. doi: https://doi.org/10.1136/bcr.01.2012.5497
15. Zhang FB, Zhang AM, Zhang ZB, Huang X, Wang XT, Dong JH. Preoperative differential diagnosis between intrahepatic biliary cystadenoma and cystadenocarcinoma: a single-center experience. *World J Gastroenterol* 2014; **20**: 12595–601. doi: https://doi.org/10.3748/wjg.v20.i35.12595
16. Dixon E, Sutherland FR, Mitchell P, McKinnon G, Nayak V. Cystadenomas of the liver: a spectrum of disease. *Can J Surg* 2001; **44**: 371–6.
17. Delis SG, Touloumis Z, Bakoyiannis A, Tassopoulos N, Paraskeva K, Athanassiou K, et al. Intrahepatic biliary cystadenoma: a need for radical resection. *Eur J Gastroenterol Hepatol* 2008; **20**: 10–14. doi: https://doi.org/10.1097/MEG.0b013e3282f16a76
18. Kim K, Choi J, Park Y, Lee W, Kim B. Biliary cystadenoma of the liver. *J Hepatobiliary Pancreat Surg* 1998; **5**: 348–52. doi: https://doi.org/10.1007/s005340050058
19. Voltaggio L, Szeto OJ, Tabbara SO. Cytologic diagnosis of hepatobiliary cystadenoma with mesenchymal stroma during intraoperative consultation: a case report. *Acta Cytol* 2010; **54**(5 Suppl): 928–32.
20. Xu MY, Shi XJ, Wan T, Liang YR, Wang HG, Zhang WZ, et al. Clinicopathological characteristics and prognostic factors of intrahepatic biliary cystadenocarcinoma. *Chin Med J* 2015; **128**: 1177–83. doi: https://doi.org/10.4103/0366-6999.156108
21. Lim JH, Zen Y, Jang KT, Kim YK, Nakanuma Y. Cyst-forming intraductal papillary neoplasm of the bile ducts: description of imaging and pathologic aspects. *AJR Am J Roentgenol* 2011; **197**: 1111–20. doi: https://doi.org/10.2214/AJR.10.6363
22. Wang X, Cai YQ, Chen YH, Liu XB. Biliary tract intraductal papillary mucinous neoplasm: report of 19 cases. *World J Gastroenterol* 2015; **21**: 4261–7. doi: https://doi.org/10.3748/wjg.v21.i14.4261
23. Minagawa N, Sato N, Mori Y, Tamura T, Higure A, Yamaguchi K. A comparison between intraductal papillary neoplasms of the biliary tract (BT-IPMNs) and intraductal papillary mucinous neoplasms of the pancreas (P-IPMNs) reveals distinct clinical manifestations and outcomes. *Eur J Surg Oncol* 2013; **39**: 554–8. doi: https://doi.org/10.1016/j.ejso.2013.02.016
24. Lim JH, Yoon KH, Kim SH, Kim HY, Lim HK, Song SY, et al. Intraductal papillary mucinous tumor of the bile ducts. *Radiographics* 2004; **24**: 53–66. doi: https://doi.org/10.1148/rg.241035002
25. Takanami K, Yamada T, Tsuda M, Takase K, Ishida K, Nakamura Y, et al. Intraductal papillary mucininous neoplasm of the bile ducts: multimodality assessment with pathologic correlation. *Abdom Imaging* 2011; **36**: 447–56. doi: https://doi.org/10.1007/s00261-010-9649-x
26. Edmondson HA. Tumors of the liver and intrahepatic bile ducts. In: *Atlas of tumor pathology, fascicle 25*. Washington DC: Armed Forces Institute of Pathology; 1958. pp. 19–29.
27. Kim YS, Rha SE, Oh SN, Jung SE, Shin YR, Choi BG, et al. Imaging findings of intrahepatic bile duct adenoma (peribiliary gland hamartoma): a case report and literature review. *Korean J Radiol* 2010; **11**: 560–5. doi: https://doi.org/10.3348/kjr.2010.11.5.560
28. Chen L, Xu MY, Chen F. Bile duct adenoma: a case report and literature review. *World J Surg Oncol* 2014; **12**: 125. doi: https://doi.org/10.1186/1477-7819-12-125
29. Moon SG, Han JK, Kim TK, Kim AY, Kim TJ, Choi BI. Biliary obstruction in metastatic disease: thin-section helical CT findings. *Abdom Imaging* 2003; **28**: 45–52. doi: https://doi.org/10.1007/s00261-001-0191-8
30. Popp JW, Schapiro RH, Warshaw AL. Extrahepatic biliary obstruction caused by metastatic breast carcinoma. *Ann Intern Med* 1979; **91**: 568–71. doi: https://doi.org/10.7326/0003-4819-91-4-568
31. Granata V, Fusco R, Catalano O, Avallone A, Leongito M, Izzo F, et al. Peribiliary liver metastases MR findings. *Med Oncol* 2017; **34**: 124. doi: https://doi.org/10.1007/s12032-017-0981-7
32. Mittal PK, Moreno CC, Kalb B, Mittal A, Camacho JC, Maddu K, et al. Primary biliary tract malignancies: mri spectrum and mimics with histopathological correlation. *Abdom Imaging* 2015; **40**: 1520–57. doi: https://doi.org/10.1007/s00261-014-0300-0
33. Washburn WK, Noda S, Lewis WD, Jenkins RL. Primary malignant melanoma of the biliary tract. *Liver Transpl Surg* 1995; **1**: 103–6. doi: https://doi.org/10.1002/lt.500010206
34. Gates J, Kane RA, Hartnell GG. Primary biliary tract malignant melanoma. *Abdom Imaging* 1996; **21**: 453–5. doi: https://doi.org/10.1007/s002619900103
35. Smith NE, Taube JM, Warczynski TM, Collier KD, Pawlik TM. Primary biliary tract melanoma: report of a case and review of the literature. *Int J Surg Case Rep* 2012; **3**: 441–4. doi: https://doi.org/10.1016/j.ijscr.2012.05.008
36. Medina V, Darnell A, Bejarano N, Falcó J, Musulen E, Martin J. Primary biliary tract malignant melanoma: us, CT, and MR findings. *Abdom Imaging* 2003; **28**: 842–6. doi: https://doi.org/10.1007/s00261-003-0051-9
37. Costello JR, Kalb B, Chundru S, Arif H, Petkovska I, Martin DR. MR imaging of benign and malignant biliary conditions. *Magn Reson Imaging Clin N Am* 2014; **22**: 467–88. doi: https://doi.org/10.1016/j.mric.2014.05.002